frontiers | Frontiers in Materials

TYPE Original Research
PUBLISHED 19 December 2022
DOI 10.3389/fmats.2022.1081858

OPEN ACCESS

EDITED BY
Ramadhansyah Putra Jaya,
Universiti Malaysia Pahang, Malaysia

REVIEWED BY
Huanan Yu,
Changsha University of Science and Technology, China
Zaid Hazim Al-Saffar,
Northern Technical University (NTU), Iraq

*CORRESPONDENCE
Xie Yuanguang,
956104362@qq.com

SPECIALTY SECTION
This article was submitted to Structural Materials, a section of the journal Frontiers in Materials

RECEIVED 27 October 2022
ACCEPTED 25 November 2022
PUBLISHED 19 December 2022

CITATION
Yi J, Yuanguang X and Zhengjia L (2022), Optimization design and performance evaluation of a novel asphalt rejuvenator.
Front. Mater. 9:1081858.
doi: 10.3389/fmats.2022.1081858

Optimization design and performance evaluation of a novel asphalt rejuvenator

Jiao Yi[1], Xie Yuanguang[1]* and Liu Zhengjia[2]

[1]Chongqing Jiaotong University, Chongqing, China, [2]Xinjiang Beixin Investment and Construction Co., Chongqing, China

The development of a regeneration agent is one of the key technologies for pavement regeneration and one of the methods to reduce carbon emissions in the transportation field, so it is very necessary to develop a regeneration agent. Based on the composition of asphalt and rejuvenator components, the optimal dosing of extraction oil, plasticizer dioctyl phthalate (DOP), and hydrogenated (carbon 9) C9 petroleum resin was determined by the response surface method, and the suitable dosing of the anti-aging agent was also designed to optimize the orthogonal experiment to prepare the ZJ-I (Zenith Yummy-Invent) rejuvenator with good overall performance. On the basis of the ZJ-I rejuvenator, dynamic shear rheology (DSR), bending beam rheometery (BBR), Fourier transform infrared spectroscopy (FTIR), atomic force microscopy (AFM), and contact angle experiments were used to investigate the effects of the ZJ-I rejuvenator dosing on the high- and low-temperature rheology, chemical structure, surface microscopic morphology, and adhesion between asphalt and aggregate of aged asphalt and to explore the regeneration effect and regeneration mechanism of the ZJ-I rejuvenator. The results showed that the ZJ-I rejuvenator formulated with 83.6% extracted oil, 15% plasticizer DOP, 1.4% hydrogenated petroleum resin, 0.6% antioxidant, and 0.4% light stabilizer has the best regeneration effect, and its optimal dosing is 7% aging degree. It can also improve the adhesion performance of asphalt and aggregate.

KEYWORDS

regenerating agent, regeneration performance, optimized design, regenerative mechanisms, adhesion performance

1 Introduction

In the background of peaking carbon dioxide emissions, carbon emissions from transportation have become a giant problem that needs to be solved urgently, and one of the main sources of carbon emissions in this field is the maintenance of roads which will generate a lot of waste asphalt materials. Under such circumstances, pavement recycling becomes one of the important measures to reduce carbon emissions. Pavement recycling is necessary for its effects in reducing resource waste, cost, and carbon emissions, and it is a way to achieve the sustainable development of the economy, society, and environment.

There are many technologies for pavement recycling, and one of the key technologies is the development of asphalt-recycling agents. The purpose of pavement recycling is to

restore the aged asphalt to the level of the original asphalt. The aged asphalt inside which the components have been out of balance and most of the aromatics and saturate are converted to asphaltenes becomes hard and easy to crack (Huang et al., 2011). According to the principle of four components of asphalt, light oil, the main component of the asphalt-recycling agent, can dissolve or disperse the content of high molecular weight (or dissolve a large number of asphaltenes) so that the components in the asphalt can be balanced and the asphalt can be restored to the original state, so as to achieve the asphalt recycling. Thus, the research on the asphalt-recycling agent is the key to achieving pavement recycling.

At present, scholars at home and abroad have carried out a lot of research on the development of rejuvenators. Yanan et al. (2022) found that waste engine oil can better improve the low-temperature cracking resistance of asphalt. AlSaffar et al. (2022) and Elio et al. (2021) found that maltose was effective in improving the low-temperature cracking resistance of asphalt and its improvement effect was close to that of the as-built asphalt. Sokolova et al. (2019) found that different plasticizers such as TBC, DOM, and DOP were able to improve the low-temperature properties of asphalt, with DOP plasticizers improving most significantly. Gómez-Mejide et al. (2018) and Han et al. (2022) also studied the effect of plasticizers on high- and low-temperature rheology and microstructure and also proposed the optimum number of plasticizers to be 7%.

Previously, it was found that materials such as waste engine oil have improved the low-temperature crack resistance of asphalt, but the best improvement was achieved by DOP plasticizers. However, DOP plasticizers can adversely affect the high-temperature shear and aging resistance of asphalt, so some materials that can improve the high temperature and aging resistance of asphalt need to be added. Nie et al. (2019) and Radzi et al. (2020) and Sharma et al. (2020) and Shao-peng et al. (2002)) found that adding hydrogenated C9 petroleum resin to plasticizers can better improve the aging resistance of asphalt. Wu et al. (2022) determined the microscopic morphology and the results proved that the addition of petroleum resin could indeed alleviate the aging of SBS-modified asphalt. Meanwhile, Zhao et al. (2022) and Yin and Pan (2022) found that the addition of antioxidants to plasticizers could improve the high-temperature performance of asphalt, which could compensate for the negative effects of plasticizers.

The aforementioned literature reveals that the addition of plasticizers, tackifiers, and antioxidants can significantly improve the performance of asphalt, such as low-temperature rheology and anti-aging properties. In order to further study the effect of these material components on asphalt properties, some scholars choose to optimize the materials by compounding, of which the use of the orthogonal design method for material compounding is one of the most widely used methods. Li et al. (2022) used the orthogonal design method to compound six base oils and five plasticizing modifiers, and the results proved that the low-temperature and adhesion properties of asphalt were significantly improved. Li et al. (2022) similarly used an orthogonal design approach to compound glycolaldehyde extraction oil with hydrogenated C9 petroleum resin, and the results demonstrated a large improvement in the low-temperature properties of asphalt.

At present, most scholars in China and abroad use the orthogonal design method to compound the rejuvenator and study the influence of rejuvenator on the aged asphalt at high temperature and its anti-aging performance. At the same time, they studied the regeneration mechanism of the rejuvenator. These studies have important contributions to the improvement of asphalt performance and the utilization ratio of reclaimed materials. However, there are still some problems with the existing rejuvenators of asphalt. Taking the commonly used configuration mode as an example, there are some defects in single matching, while the orthogonal design method which is used in compounding frequently is not that accurate.

To address the existing problems, this paper develops an inexpensive rejuvenator with good overall performance based on a rejuvenator formulation optimization design. According to the research of previous scholars, it can be found that the combination of three materials, namely, glyoxal extracted oil, plasticizer DOP, and hydrogenated C9 petroleum resin, can improve the low-temperature rheology, anti-aging, and adhesion of asphalt and aggregate. In order to improve the high-temperature shear resistance of asphalt, some anti-aging materials were added to the rejuvenator. First, the response surface method was used to determine the optimal amount of extracted oil, plasticizer DOP, and hydrogenated C9 petroleum resin, and then the orthogonal design method was used to determine the optimal amount of anti-aging materials so that a ZJ-I type rejuvenator was prepared. Next, dynamic shear rheology (DSR), bending creep stiffness, Fourier transform infrared spectroscopy (FTIR), atomic force microscopy (AFM), and contact angle tests were conducted to verify the regeneration performance of the ZJ-I rejuvenator and to investigate the regeneration mechanism of the ZJ-I rejuvenator. The effect of the ZJ-I rejuvenator on the road performance of asphalt and asphalt mixes was analyzed from a macro and micro perspectives. The resulting technology roadmap is shown in Figure 1.

2 Materials and methods of experiment

2.1 Raw materials

2.1.1 Asphalt

In this paper, heavy traffic No. 70 Grade A asphalt was used as the base asphalt, and the base asphalt was aged in a

TABLE 1 Basic performances of the three kinds of asphalt.

Index	Unit	Base asphalt	Self-made aged asphalt	Extracted aged asphalt	Specification requirement	Test method
Penetration (25°C)	0.1 mm	67.16	34	29	60–80	T0604
10°C ductility	mm	389	80	45	>200	T0605
Softening point	°C	49.3	62	68	>46	T0606

TABLE 2 Base oil component.

Index	Test results			Specification requirement	Test method
	Extraction oil	Aromatic oil	Rubber oil		
Density (g/cm3 20°C)	1.02	1.05	0.847	Actual test	GB/T1884
Flashpoint (°C)	240	220	224	>60	GB/T267

TABLE 3 Plasticizer component.

Index	Test results			Specification requirement	Test method
	TBC	Soybean oil	DOP		
Density (20°C)	1.042	0.989	0.982	Actual test	GB/T1884
Flashpoint (°C)	195	260	196	>60	GB/T267

TABLE 4 Tackifier component.

Index	Test results			Specification requirement	Test method
	Terpene resin T-100	C5 petroleum resin	Hydrogenated C9 petroleum resin		
Molecular number	1,460	1,180	1,350	Actual test	GB/T21864
Softening point(°C)	130	101	118	>46	T0606

TABLE 5 Anti-aging component.

Index	Test results		Specification requirement	Test method
	Antioxidant 1,010	Light stabilizer 770		
Molecular number	1,178	479	Actual test	GB/T21864
Flashpoint (°C)	297	258	>60	GB/T267

rotating film oven for 5 h to obtain the aged asphalt samples. The basic properties of the aged asphalt were tested and found to be close to those of the extracted aged asphalt. The basic properties of the matrix asphalt, aged asphalt (homemade), and aged asphalt (extracted) are shown in Table 1.

TABLE 6 Experiment design table.

Code	X_1	X_2	X_3
1	75	40	1
2	75	25	3
3	90	40	3
4	90	25	1
5	75	25	3
6	60	25	1
7	60	10	3
8	75	10	5
9	60	25	5
10	75	25	3
11	90	25	5
12	75	10	1
13	60	40	3
14	75	25	3
15	90	10	3
16	75	40	5
17	75	25	3

2.1.2 Raw materials of the rejuvenator

According to the related literature, the elements making rejuvenators include a base oil component, plasticizer component, tackifying component, and anti-aging component. The basic performances of materials of various components are shown in Table 2, Table 3, Table 4, and Table 5.

2.2 Optimal design method of the rejuvenator

2.2.1 Proportion design of the rejuvenator

We usually use the response surface methodology (RSM) and orthogonal design to design the proportion of the rejuvenator.

1) Response surface methodology

The response surface methodology, one of the methods to determine the optimal content of materials, has higher accuracy in proportion than the orthogonal design methodology. First, it uses reasonable experimental design methods and obtains certain data through experiments. Then, the multiple quadratic regression equation is used to fit the functional relationship between factors and response values. Finally, the analysis of the regression equation is used to seek the optimal process parameters and solve multivariable problems. Therefore, here, the text response surface methodology is used to determine the optimal dosage of extract oil, plasticizer, and hydrogenated C9 petroleum resin. In the experiment, here are three variables, X1 (extract oil), X2 (plasticizer), and X3 (hydrogenated C9 petroleum resin). Correspondingly, the three response values are penetration (Y1), 10°C ductility (Y2), and softening point (Y3). Since there are three factors and levels, the design of the experiment is based on three factors and three levels. The Box–Behnken design (BBD) method in the response surface method is selected to design the experiment, so 17 groups of experiments are required for three factors and three levels. To distinguish the materials, the extracted oil is marked as X1, the plasticizer DOP is marked as X2, and the hydrogenated C9 petroleum resin is marked as X3. The response surface design table is shown in Table 6.

TABLE 7 Orthogonal experimental design table.

Order	Antioxidant D(%)	Light stabilizer F(%)
1	0.4 (D1)	0.4 (F1)
2	0.4 (D1)	0.6 (F2)
3	0.4 (D1)	0.8 (F3)
4	0.6 (D2)	0.4 (F1)
5	0.6 (D2)	0.6 (F2)
6	0.6 (D2)	0.8 (F3)
7	0.8 (D3)	0.4 (F1)
8	0.8 (D3)	0.6 (F2)
9	0.8 (D3)	0.8 (F3)

2) Orthogonal design

The method of the orthogonal design is used to determine the optimal dosage of anti-aging materials. Because there are altogether two anti-aging materials and each has three optimal dosages, the orthogonal experimental design conduct nine groups of experiments by adopting two factors and three level. In order to distinguish the materials, the antioxidant is marked as D, and the light stabilizer is marked as F. The orthogonal experimental design table is shown in Table 7.

2.2.2 Preparation of the self-made rejuvenator and recycled asphalt

To make the rejuvenator, first, the extracted oil, plasticizer DOP, hydrogenated C9 petroleum resin, antioxidant, and light stabilizer should be weighed according to the proportion. Then, the extracted oil is put in a water bath with a temperature of 120°C. Next, the plasticizer DOP is added into it for stirring with a high-speed shearing machine with a rotation speed of 2,000 r/

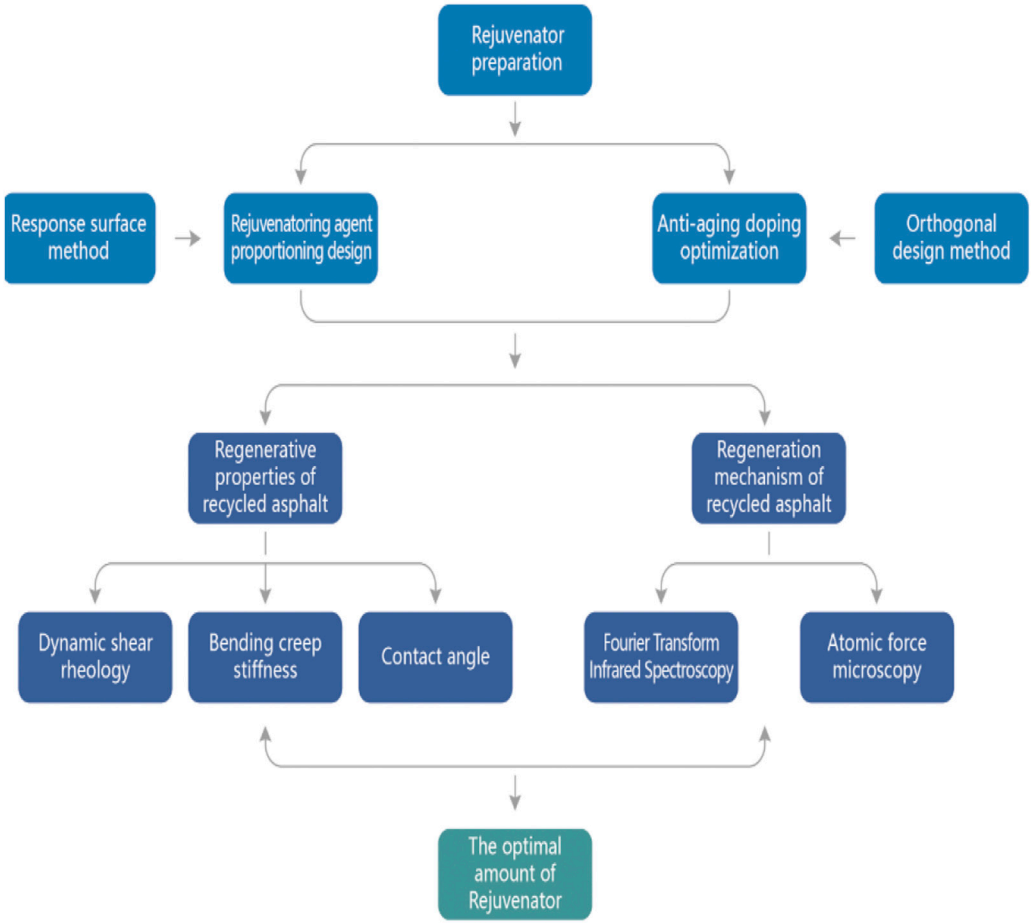

FIGURE 1
Thesis technology roadmap.

min and stirred it for 5 min. Then, the temperature is increased to 150°C and the rotation speed is improved to 5,000 r/min. After that, C9 petroleum resin, antioxidant, and light stabilizer are added into the water bath in order and stirred it for 14 min, 8 min, and 8 min, respectively. Finally, the ZJ-I type rejuvenator has been made and the prepared rejuvenator is put in a vessel. To make the recycled asphalt, first, the aged asphalt is heated in a 130°C oil bath until it melts. Then, 4% ZJ-I type rejuvenator, 7% ZJ-I type rejuvenator, 10% ZJ-I type rejuvenator, and 7% (Roughness American) RA-5 rejuvenator are added (a commercial rejuvenator, as the control group of the self-made rejuvenator, the optimal dosage of the rejuvenator has been determined to be 7% in the preliminary test) to aged asphalt and used the shearing machine for high-speed shearing at 2,500 r/min for 8 min. In this way, different kinds of dosages of recycled asphalt are made. The process of making the self-rejuvenator goes as follows (Figure 2, Figure 3).

2.3 Test methods of asphalt performance

2.3.1 DSR

DSR tests of aged asphalt, original asphalt, and recycled asphalt are carried out with a dynamic shear rheometer. The temperature scanning is conducted according to the procedure specified in T0628-2011. The test temperature is from 50°C to 75°C and there will be a temperature scanning when the temperature increases by 5°C every time. The two indicators tested are the complex modulus G * and the phase angle δ. G * reflects the permanent deformation resistance of asphalt and is related to the stiffness of asphalt. The larger the G *, the greater the stiffness and the stronger the deformation resistance of asphalt. δ is related to asphalt viscoelasticity. The smaller the δ, the closer it is to elastic materials, and on the contrary, the closer it is to viscous materials.

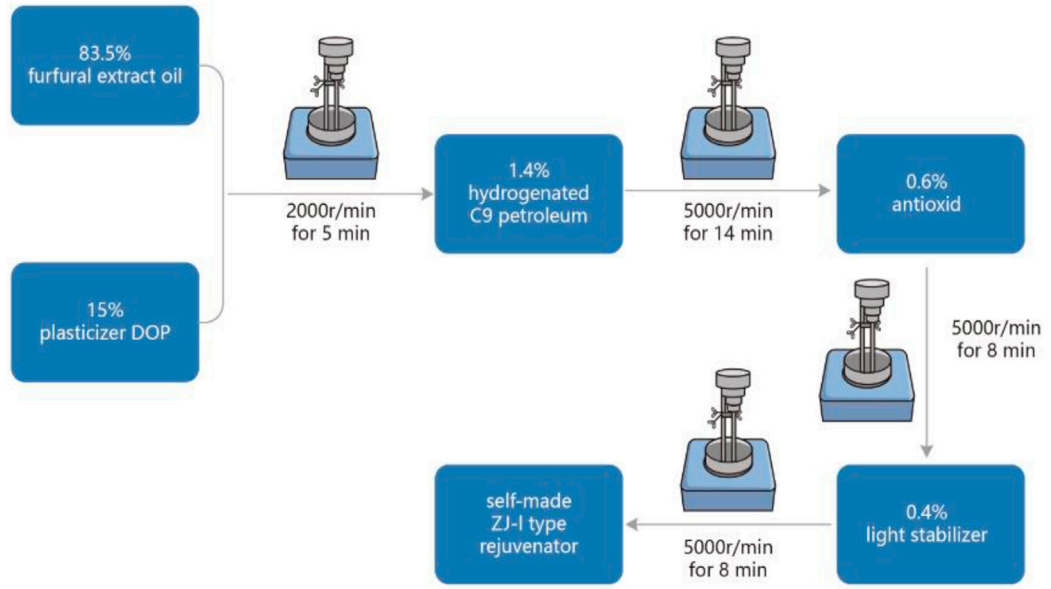

FIGURE 2
Process diagram of rejuvenator preparation.

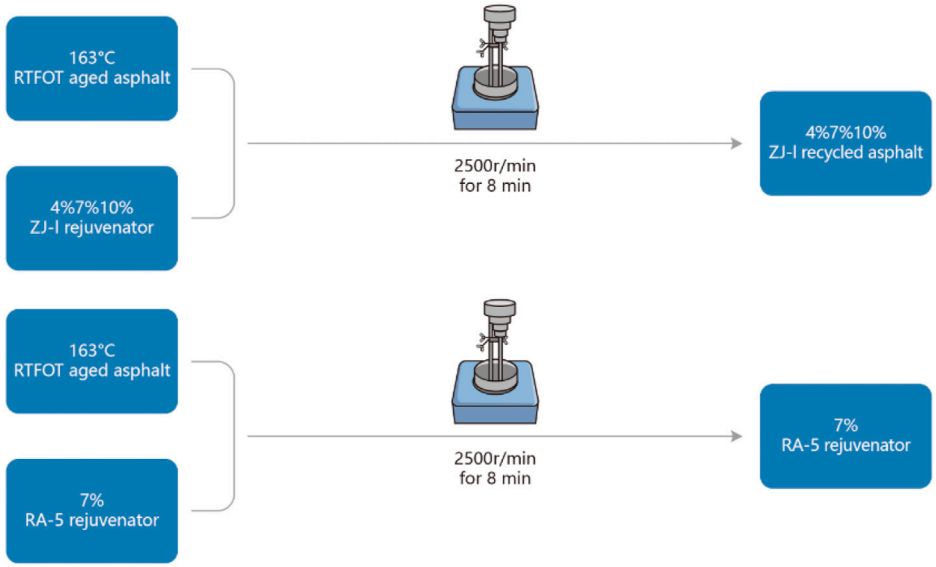

FIGURE 3
Preparation process of recycled asphalt.

2.3.2 BBR

According to T0627 in JTGE 20–2011, the 60 s bending creep stiffness modulus S value of asphalt and creep rate m value are used to evaluate the low-temperature performance of aged asphalt, original asphalt, and recycled asphalt. In the test, the 60 s bending creep stiffness modulus S value means that the larger the creep stiffness modulus of asphalt, the easier the asphalt is to crack at low temperature, and the creep rate M value means that the higher the creep rate of asphalt, the better the stress relaxation ability, and the better the low-temperature crack

TABLE 8 Surface energy parameters of three test liquids.

Liquid	γ	γ^d	γ^p
Distilled water	72.80	21.80	51.00
Ethylene glycol	48.00	29.00	19.00
Formamide	58.00	39.00	19.00

resistance of asphalt. The size of the test samples is 127 mm × 6.35 mm × 12.7 mm and the test temperature is -12°C,-18°C, and -24°C.

2.3.3 FTIR

Here in the paper, infrared spectra of base asphalt, aged asphalt, and recycled asphalt are measured by using infrared spectrometers. By comparing and analyzing the infrared spectra, the changes in chemical characteristic functional groups of asphalt can be shown after adding the self-made rejuvenator. In the experiment, the scanning range of the infrared spectrometer is 500–4000cm^{-1}, the number of scans is 32 times, and the resolution is 4cm^{-1}.

2.3.4 AFM

There have been a great number of scholars, who have adopted various microscopic analysis methods to analyze the mechanism of asphalt regeneration in the aspect of asphalt regeneration and recycled asphalt mixture. Atomic force microscopy has proven to be an effective microscopic technique for observing the microscopic morphology of asphalt. Hence in this experiment, atomic force microscopy is used to observe the microstructure of asphalt and study the effect of self-made rejuvenators on the aging and regeneration of asphalt.

The tapping mode of atomic force microscopy has been used in this experiment. The AFM uses a probe with a size of 0.4 N/m. In this experiment, the scanning range is 20 μ m × 20 μ m and the scanning frequency is 512. According to the documents, to produce the AFM, first, a little asphalt is dipped with a glass rod and dropped it in the center of the slide. Then, put it into the baking oven to heat for 15 min. Eventually, the AFM sample has been made when the asphalt sample flow into a thin film on the glass slide.

2.3.5 Contact angle test

The adhesion between asphalt and aggregate affects the stability of the asphalt mixture. Therefore, it is necessary to explore the index of adhesiveness. In this section, the contact angle test is used to determine the contact angles of original asphalt, aged asphalt, and recycled asphalt. Then, the surface free energy and adhesiveness of various asphalts are calculated by using the correlation formula of the surface free energy theory. Hence in this way, it is used to determine the effect of the rejuvenator on the adhesion of the asphalt to the aggregate. Surface energy parameters of the three liquids with known surface free energy required for the contact angle test are shown in Table 8. The formula for adhesiveness is

TABLE 9 Test design and results.

Order	X_1	X_2	X_3	Y_1	Y_2	Y_3
1	75	40	1	59	437	45
2	75	25	3	55	337	47.4
3	90	40	3	61.6	560	44.3
4	90	25	1	57.6	460	45.5
5	75	25	3	55	337	47.4
6	60	25	1	51.1	292	47
7	60	10	3	49.1	192	49.8
8	75	10	5	50	237	49.5
9	60	25	5	51	262	47.3
10	75	25	3	55	337	47.6
11	90	25	5	57	452	45.7
12	75	10	1	50.7	345	49.3
13	60	40	3	52	362	45.9
14	75	25	3	55	337	47.4
15	90	10	3	56	352	49
16	75	40	5	58.1	429	45.2
17	75	25	3	55	337	47.4

$$W_a = \gamma_l (1 + \cos\theta) \tag{2.1}$$

In the formula, W_a—adhesiveness (mJ/m^2); γ_l γ_l—surface energy of the asphalt material (mJ/m^2); and θ—contact angle between the asphalt material and aggregate (°).

3 Results and discussion

3.1 Proportion design of the rejuvenator using the response surface method

See Table 9 for the results obtained by the response surface method.

Next, according to the obtained test data, we take the softening point value of the response value as an example, simulate the equation, and test the significance with the help of Expert-Design software (Liu et al., 2012; Huang et al., 2021; Al-Saffar et al., 2022). The remaining two response value analysis methods and processes are the same. The results are shown in Table 10.

A significant model means that a response value has a large effect on several variables, and the predicted data have very little difference from the measured data. If you want the

TABLE 10 Numerical analysis of the softening point.

Project	Square sum	Freedom	Mean square deviation	F value	*p* value	Significance
Model	43.89	9	4.88	361.20	<0.0001	Significant
Pumping oil dosage	3.78	1	3.78	280.09	<0.0001	—
DOP dosage	36.98	1	36.98	2,739.26	0.0002	—
Hydrogenated C9 resin dosage	0.10	1	0.10	7.50	0.0290	—

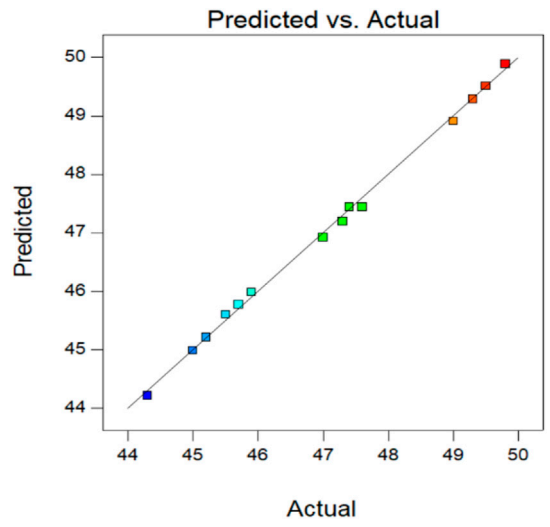

FIGURE 4
Distribution of measured and predicted softening point values.

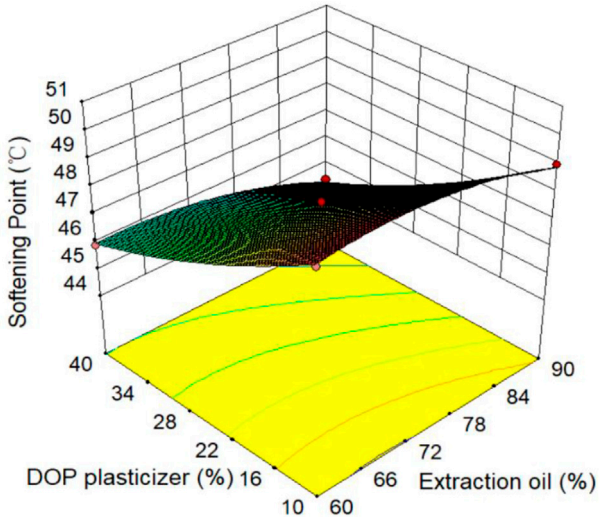

FIGURE 5
Extraction oil with DOP plasticizer.

model to be significant, the *p* value in the model must be less than 0.05. According to the table, the model *p* value of the softening point indicator is < 0.0001 < 0.05, so the model is significant. The regression equation of the softening point was also calculated according to the software:

$$Y = 47.44 - 0.69X_1 - 2.15X_2 + 0.11X_3 - 0.2X_1X_2 - 0.025X_1X_3 + 0.000X_2X_3 - 0.53X_1^2 + 0.34X_2^2 - 0.53X_3^2.$$

In the aforementioned formula, X1 is the content of extracted oil, X2 is the content of plasticizer DOP, and X3 is the content of hydrogenated C9 petroleum resin.

Through software analysis, we get that the correlation coefficient of the regression equation of the softening point is $R^2 = 0.9968$, which indicates that the response surface method is reasonable in predicting the softening point. The following figure intuitively shows the difference between the predicted and measured softening point values (Figure 4).

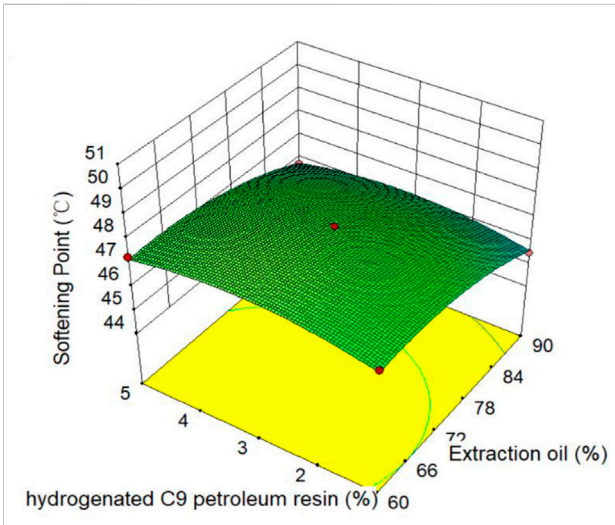

FIGURE 6
Extracted oil with hydrogenated C9 petroleum resin.

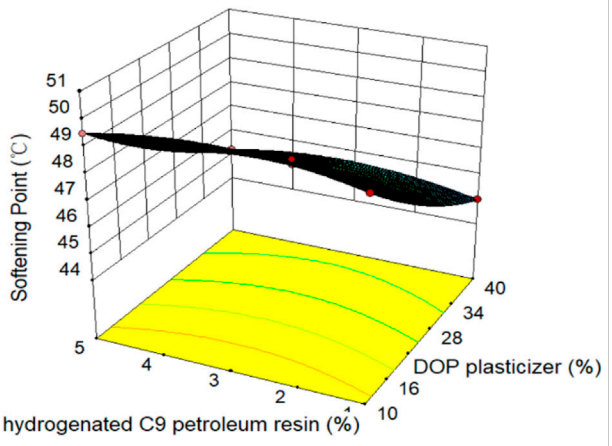

FIGURE 7
DOP plasticizer with hydrogenated C9 petroleum resin.

As can be seen from Figure 4, all the points fall on the diagonal line, which indicates that the measured results are in good agreement with the simulation results, indicating that the model used is reasonable and the reliability of the fitted equations is good. In addition, the surface relationship between the softening point value and the extracted oil, plasticizer, and hydrogenated C9 resin is shown in Figure 5, Figure 6, and Figure 7.

According to Figures 5–7, under the condition that the content of hydrogenated C9 petroleum resin is unchanged, the softening point value decreases with the increase of plasticizer DOP and extracted oil, and the influence of the content of extracted oil and plasticizer DOP on the softening point is relatively small. Under the condition that the content of extracted oil is fixed, the softening point value increases with the increase of the content of hydrogenated C9 petroleum resin and decreases with the increase of the content of plasticizer DOP. In particular, the range of change of the softening point value with the content of plasticizer DOP is significantly higher than that of hydrogenated C9 petroleum resin. When the DOP content of the plasticizer is constant, the softening point value increases with the increase of the content of hydrogenated C9 petroleum resin and decreases with the increase of the content of extracted oil. In particular, the range of change of the softening point value with the content of extracted oil is slightly lower than that of hydrogenated C9 petroleum resin.

It can be concluded that the influence intensity of three factors on the softening point value is: DOP > hydrogenated C9 petroleum resin > extracted oil.

Similarly, the other two response values can be analyzed. The influence intensity of the three factors on the penetration value is: extracted oil > DOP > hydrogenated C9 petroleum resin. The strength of influence on ductility is DOP > extracted oil > hydrogenated C9 petroleum resin. In terms of the influence degree, DOP and extracted oil have a significant influence on the factors, so the content of extracted oil and DOP will be more than that of hydrogenated C9 petroleum resin.

Therefore, the optimal ratio of the main materials of the rejuvenator was obtained after optimization by the response surface method: 83.6% extraction oil, 15% plasticizer DOP, and 1.4% hydrogenated petroleum resin.

3.2 Optimization of anti-aging agent materials by the orthogonal test

See Table 11 for test results of the orthogonal test design.

The data in the aforementioned table are analyzed, and the range of each indicator is calculated. Taking the mass loss range as an example, the calculation results are shown in Table 12. Using the same method, the remaining penetration and the range of penetration ratio can be analyzed.

According to the mass loss extreme difference analysis table, we can see that level 1, level 2, and level 3 of antioxidants are −0.21, −0.25, and −0.35, respectively, and level 1, level 2, and level 3 of the light stabilizer are −0.22, −0.24, and −0.30, respectively, because the smaller the mass loss, the better the anti-aging ability, so we need to choose the one with the smallest mass loss extreme difference value. The lowest mass loss polarization among the antioxidants is −0.21, and the lowest mass loss polarization among the light stabilizers is −0.22, so it can be seen that the optimal combination of mass loss polarization is D1F1. Similarly, the optimal combination from the needle penetration polarization analysis is D2F1 and D2F3.

In summary, from the extreme difference analysis table of mass loss, needle penetration, and needle penetration ratio, it can be seen that the doping amount marked as D2 affects both needle penetration and needle penetration ratio, and the doping amount marked as F1 also affects both mass loss and needle penetration, and these two doping amounts have significant effects on the test, so the final combination is D2F1, where D2 represents the data of antioxidant level 2, and F1 represents the data of light stabilizer level 1, according to Table 7, D2 is 0.6% and F1 is 0.4%.

Finally, the optimal combination of homemade new rejuvenators obtained by the response surface method, and the orthogonal design is 83.6% extraction oil, 15% plasticizer DOP, 1.4% hydrogenated petroleum resin, 0.6% antioxidant, and 0.4% light stabilizer.

3.3 DSR

After dynamic shear change (Jaafar et al., 2021) recycled asphalt, original asphalt, and aged asphalt with different

TABLE 11 Test and test results.

序列	Keywords antioxidant (D)	Light stabilizer (F)	Mass loss rate	Penetration	Penetration ratio
单位	%	%	%	0.1 mm	%
1	0.4 (D1)	0.4 (F1)	−0.15	57.9	83%
2	0.4 (D1)	0.6 (F2)	−0.26	60.2	75%
3	0.4 (D1)	0.8 (F3)	−0.22	64.9	78%
4	0.6 (D2)	0.4 (F1)	−0.25	62.8	77%
5	0.6 (D2)	0.6 (F2)	−0.18	68.5	79%
6	0.6 (D2)	0.8 (F3)	−0.32	58.2	85%
7	0.8 (D3)	0.4 (F1)	−0.27	67.1	72%
8	0.8 (D3)	0.6 (F2)	−0.29	53.5	82%
9	0.8 (D3)	0.8 (F3)	−0.35	52.3	80%

TABLE 12 Analysis of the quality loss range.

Object	Level	Keywords antioxidant	Light stabilizer
K value	1	−0.63	−0.67
	2	−0.75	−0.73
	3	−0.91	−0.89
K average value	1	−0.21	−0.22
	2	−0.25	−0.24
	3	−0.30	−0.30
Best level		1	1
R		0.09	0.08

rejuvenators, the relevant data chart is obtained, as shown in Figure 8.

According to Figure 8, the rutting factor G/sinδ and complex modulus of various asphalts gradually decrease with the increase of temperature, while the phase angle increases. Moreover, when the temperature is 75°C, there is almost no difference in the complex modulus, phase angle, and rutting factor of various asphalts. In particular, at the same temperature, the rutting factor and complex modulus of asphalt after aging are higher than other asphalts, and the phase angle of aged asphalt is lower than other asphalt. After adding the rejuvenator, the rutting factor and complex modulus of the regenerated asphalt decrease with the increase of the rejuvenator content, but the rutting factor and complex modulus of recycled asphalt decreased slowly and were both higher than those of the original asphalt, while the phase angle of the regenerated asphalt increases with the increase of the rejuvenator, but both are lower than the original asphalt. In addition, the rutting factor of the ZJ-I recycled asphalt is smaller than that of RA-5 recycled asphalt when the content of the rejuvenator is the same as 7%.

The main reason for this phenomenon is that the increase in temperature makes the asphalt increase in volume and internal void volume, which increases the intermolecular spacing, decreases the intermolecular forces, decreases the asphalt's resistance to deformation, and gradually transforms the asphalt from an elastomer to a viscous body, thus making the complex modulus of all types of asphalt decrease while the phase angle increases (Zhu et al., 2017). Since the rutting factor of asphalt is derived from the equation G*/sin?, according to the equation, the rutting factor of asphalt is proportional to the complex modulus, and therefore the rutting factor decreases.

Since all types of asphalts are exposed to excessively high temperatures for an extended period of time, their molecular compositions may remain constant, making the variation in their high-temperature rheology index minimal. However, asphalt

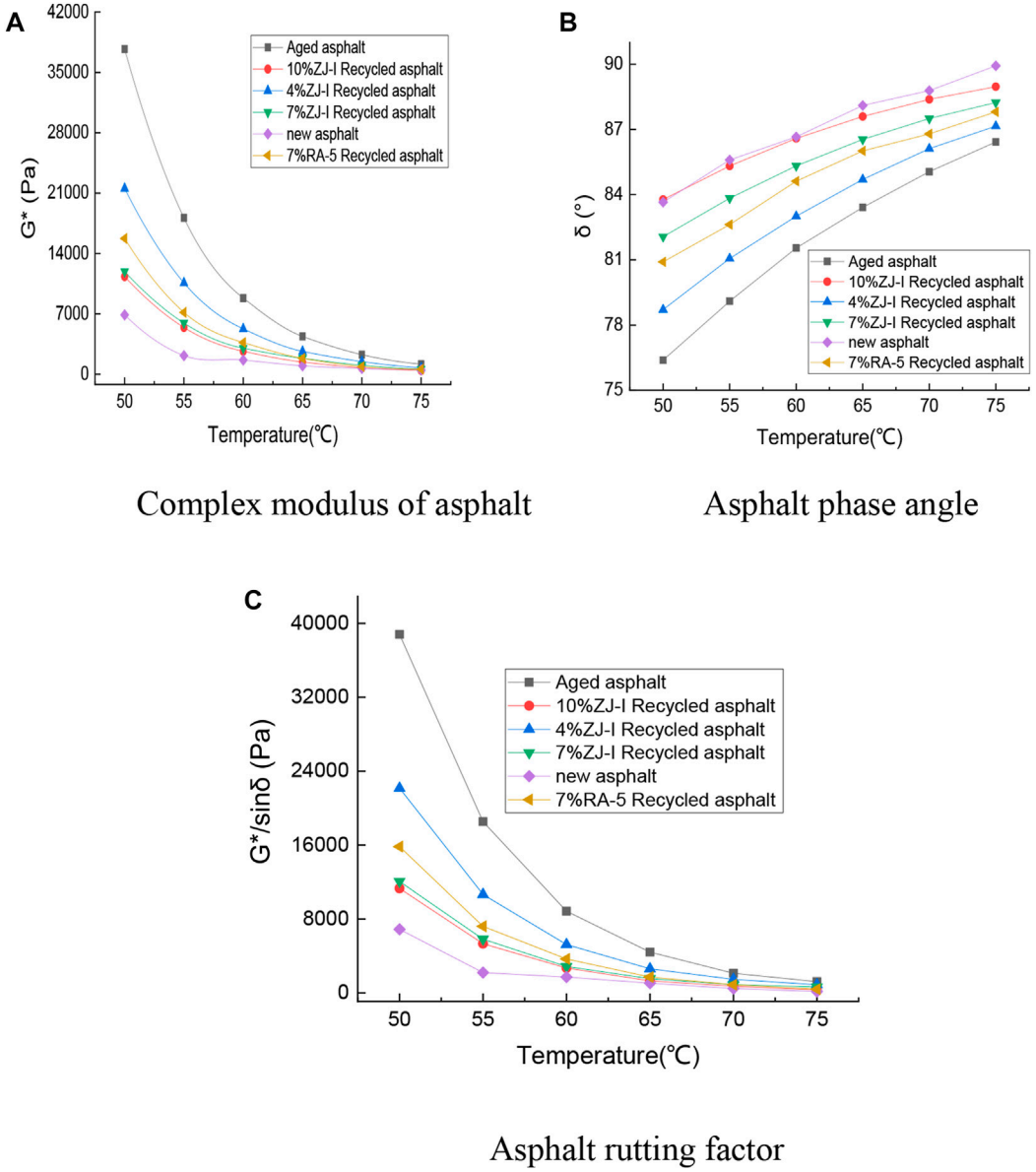

FIGURE 8
High-temperature rheological index of asphalt.

gradually hardens after thermal-oxidative aging, and the elastic recovery ability is enhanced while the viscous component is reduced, so the complex modulus and rutting factor of asphalt are enhanced while the phase angle is reduced, which makes the high-temperature shear resistance of asphalt improve (Wang et al., 2014).

The rejuvenator has the function of dissolving and softening asphalt, so after adding the rejuvenator, asphalt becomes softer and gradually shifts from the elastic state to the viscous state. Thus, the rutting factor and complex modulus of the recycled asphalt are reduced to a certain extent, and the phase angle gradually increases. As the amount of the rejuvenator is increased, the asphalt becomes closer to the viscous body, resulting in a smaller rutting factor and complex modulus, and a larger phase angle.

In addition, due to the limited function of the regenerating agent to dissolve and soften the asphalt, the elastic component of the regenerated asphalt is always higher than the original asphalt, but the elastic component of the ZJ-I regenerated asphalt is lower than the RA-5 regenerated asphalt. Therefore, the rutting factor of the ZJ-I recycled asphalt is lower than the RA-5 recycled asphalt but higher than the original asphalt.

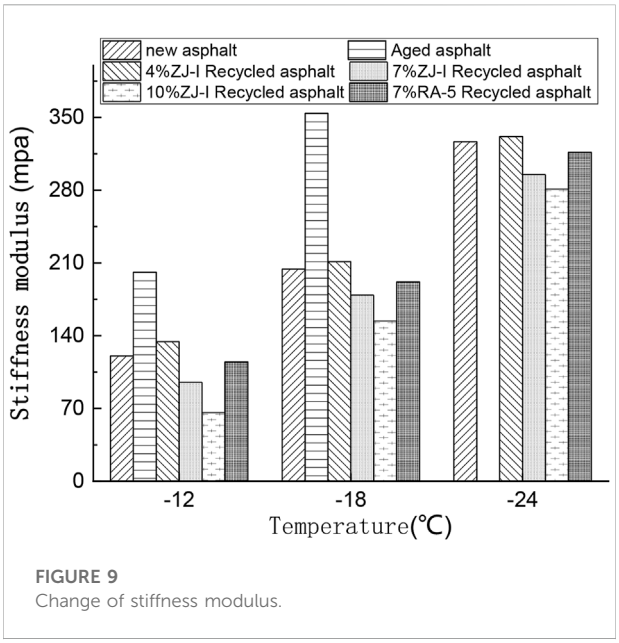

FIGURE 9
Change of stiffness modulus.

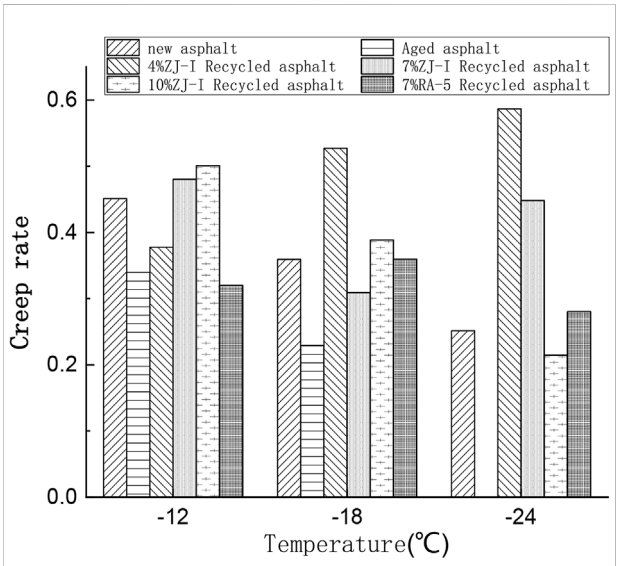

FIGURE 10
Change diagram of the creep rate.

3.4 BBR

After the low-temperature rheology of recycled asphalt, original asphalt, and aged asphalt with different rejuvenators, the creep stiffness modulus data in Figure 9 and creep rate data in Figure 10 are obtained.

According to Figure 9, the stiffness modulus of various asphalts increases in varying degrees with the decrease in temperature. When the temperature is the same, the stiffness modulus of asphalt increases after aging. The stiffness modulus of recycled asphalt decreases after adding a rejuvenator. When the amount of rejuvenator increases, the stiffness modulus of asphalt becomes smaller and smaller. When the content of the ZJ-I rejuvenator added is greater than or equal to 7%, the stiffness modulus of asphalt is smaller than the original asphalt, and 7% RA-5 recycled asphalt.

The reason for these patterns is that the lower temperature leads to an increase in the modulus of elasticity of the asphalt, which makes the asphalt more brittle, thus increasing the creep modulus. Under the same temperature conditions, asphalt gradually hardens after thermal-oxidative aging, and the complex modulus and rutting factor of asphalt are enhanced, so the strength of asphalt becomes larger, which in turn makes the creep strength modulus of aging asphalt also becoming larger (Walubita Lubinda et al., 2021).

The regenerating agent has the function of dissolving and softening asphalt, so after adding regenerating agent, it can make asphalt soft, which can promote the mobility of asphalt molecules, reduce the modulus of stiffness, and enhance the resistance of the asphalt to low-temperature cracking, the more the amount of regenerating agent, the stronger the mobility of asphalt molecules, so the asphalt" low-temperature cracking resistance is better. Therefore, the ZJ-I rejuvenator light component content is more than the RA-5 rejuvenator, so the ability of ZJ-I rejuvenator to dissolve and soften aging asphalt is stronger than the RA-5 rejuvenator, meaning that in the case of the same rejuvenator dose, the ZJ-I rejuvenated asphalt modulus is less than RA-5 rejuvenated asphalt.

According to Figure 10, the creep rate of all asphalts decreases in varying degrees with the decrease in temperature. At the same temperature, the creep rate of asphalt decreases after aging. The creep rate of recycled asphalt increases with the addition of a rejuvenator. With the increase of the rejuvenator content, the creep rate of recycled asphalt also increases. When the content of the ZJ-I rejuvenator added is 7% or more, the creep rate of asphalt is larger than that of original asphalt and 7% RA-5 regenerated asphalt.

The reason for this law is that the asphalt is in a glassy state at low temperatures, the asphalt molecular chains are almost frozen and cannot move quickly, and as the temperature drops the stress relaxation capacity of asphalt also decreases, so the creep rate of all asphalt decreases. Under the same temperature conditions, asphalt gradually hardens after aging, resulting in the increase of asphalt stiffness, the stress relaxation time will also become longer, resulting in a gradual decrease in stress and creep rate , asphalt easily becomes brittle, and its resistance to low-temperature cracking performance will be poor (Al-Saffar et al., 2021; Wu and Dai, 2022).

However, after adding the rejuvenator, the rejuvenator has the function of dissolving and softening asphalt, enhancing the mobility of asphalt molecules, the rate of asphalt release temperature stress is accelerated, the creep rate becomes

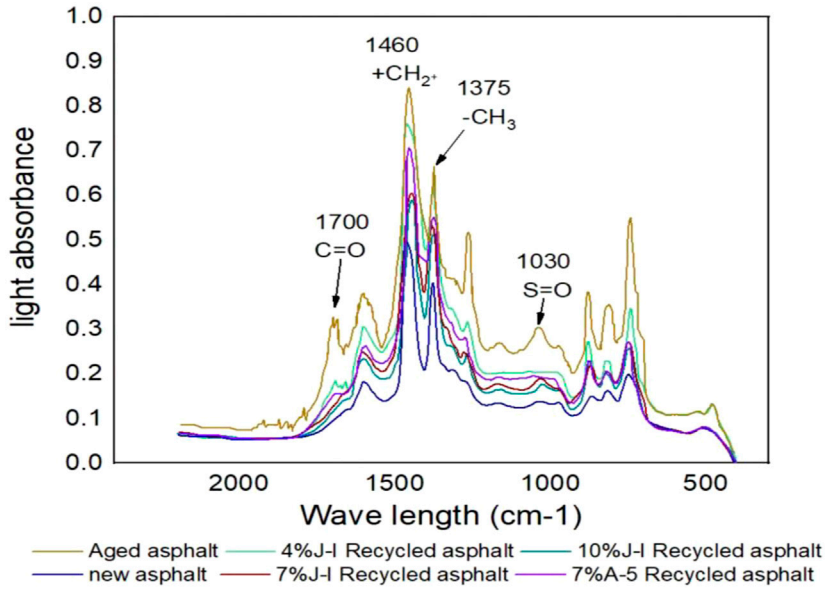

FIGURE 11
Infrared spectrum of various asphalts.

TABLE 13 $I_{C=O}$ and $I_{S=O}$ index data of the four asphalts.

Sample	New asphalt	Aged asphalt	Recycled asphalt			
			4% ZJ-I	7% ZJ-I	10% ZJ-I	7% RA-5
IS= =	0.018	0.046	0.034	0.028	0.024	0.031
IC= =	0.000	0.026	0.023	0.015	0.011	0.019

larger, and asphalt low temperature crack resistance is enhanced. More regenerating agent means quicker asphalt molecular movement, greater mobility, and a higher creep rate for recycled asphalt.

In addition, the light component content of the ZJ-I rejuvenator is more than that of the RA-5 rejuvenator, so the ability of the ZJ-I rejuvenator to dissolve and soften asphalt is stronger than that of the RA-5 rejuvenator, so the effect of the ZJ-I rejuvenator on the low-temperature crack resistance of asphalt is better than that of the RA-5 rejuvenator.

In summary, the addition of the ZJ-I rejuvenator to resist the low-temperature cracking performance of asphalt is very significant, and the improvement effect is higher than the RA-5 rejuvenator.

3.5 FTIR

In this section, infrared spectrometers are used to observe the changes in the chemical structures of recycled asphalt, aged asphalt, and base asphalt. Observe Figure 11 for the obtained infrared spectrogram. At the same time, we use the calculation formula of the two evaluation indexes of the infrared spectrum: carbonyl ($I_{C=O}$) and sulfoxide ($I_{S=O}$), as shown in Table 13.

Looking at the aforementioned figure, it is found that the positions of characteristic absorption peaks of various asphalts are roughly the same, but the intensity of absorption peaks has changed, which indicates that there is physical dissolution but no chemical reaction between aged asphalts and added rejuvenators. At the same time, there are obvious absorption peaks at 1,700 cm^{-1}, 11,00 m^{-1}, 11,60 m^{--1}, 11,75 m^{-1}, and 11,30 m^{-1} referring to the description of the infrared characteristic absorption peak position of common functional groups, it can be concluded that 11,00 m^{-1} belongs to the C = C stretching vibration of the aromatic ring; 11,60 m^{--1} and 1375cm^{--1} belong to the C-H deformation vibration of methylene (- CH2) and (-CH3), respectively; 11,30 m^{-1} belongs to the stretching vibration of sulfoxide group S = O; and 1,700 cm^{-1} belongs to the stretching vibration of carbonyl C=O (Xiao et al., 2018). When asphalt is aged, the absorption peak intensities of sulfoxide group S = O at

11,30 m^{-1} and carbonyl group C = O at 1,700 m^{-1} increase obviously, but decrease obviously after adding a rejuvenator. With the increasing rejuvenator content, the absorption peak intensities of sulfoxide group S = O at 11,30 m^{-1} and carbonyl group C = O at 1,700 m^{-1} decrease continuously. It can be deduced that the absorption peaks of sulfoxide group S = O and carbonyl group C = O have a significant influence on asphalt. Therefore, the sulfoxide group and carbonyl group can be used as the most critical parameters to evaluate the aging degree.

In order to further verify the effect of adding rejuvenators on the functional groups of aged asphalt, sulfoxide group index ($I_{s=o}$), and carbonyl group index ($I_{c=o}$) are introduced in this paper. See Table 13 for the calculation results.

By observing Table 13, it is found that for the original asphalt, $I_{C=O}$ and $I_{S=O}$ indexes increase significantly after asphalt aging. After adding rejuvenators, the $I_{C=O}$ and $I_{S=O}$ indexes of aged asphalt gradually decrease, and with the increase of rejuvenators, the $I_{C=O}$ and $I_{S=O}$ indexes of aged asphalt decrease more and more. When the amount of the rejuvenator is 10%, the aging asphalt is closest to the index of the original asphalt, but it cannot reach the level of the original asphalt.

The reason for this pattern is that after thermal-oxidative aging of asphalt, the long-chain alkyl group inside the asphalt undergoes chemical bond breakage, and after the breakage, small molecular weight free radicals are generated, but the free radicals are easily oxidized and combined with oxygen elements to form various types of functional groups at the breakage, among which the combination with free sulfur elements polymerizes under the action of oxygen elements to generate large molecular weight polar sulfoxide (S=O) functional groups, while the alkanes at the breaks polymerize with oxygen to form large molecular weight polar carbonyl (C=O) functional groups (Gao and Wang, 2016). In this way, the asphalt molecules continuously undergo chain breaking and polymerization reactions, generating more large molecules of the sulfoxide and carbonyl functional groups, resulting in increased intermolecular forces and reduced mobility, increased stiffness and complex modulus, and reduced phase angle and longer stress relaxation time, which in turn leads to a gradual decrease in stress and creep rate, and ultimately results in a significant increase in $I_{C=O}$ and $I_{S=O}$ indicators after asphalt aging, as well as the asphalt" high-temperature shear ability is enhanced, and low-temperature crack resistance is weakened.

After adding the rejuvenator, the rejuvenator supplements the long-chain alkyl, effectively inhibiting the generation of free radicals, while the aging C=O bond (carbonyl) and S=O bond (sulfoxide) are also easily reduced to C=C bond, S= = bond, *etc.* by some reducing substances in the rejuvenator, which makes the large molecular weight gradually migrate to the small molecular weight, i.e., the large molecular weight carbonyl and sulfoxide and other polar functional groups are gradually decreasing and the more amount of regeneration agent, the faster the proportion of large molecules decreases, making the asphalt molecular mobility and weakening of the force, which in turn reduces the asphalt complex modulus, phase angle increases at the same time the asphalt release temperature stress rate is also accelerated, creep rate becomes larger, and finally make the aging asphalt $I_{C\ =}$ and $I_{S\ =}$ indexes also decreases more and asphalt low-temperature cracking resistance and high-temperature cracking resistance performance is enhanced and weakened.

In addition, the biggest difference between recycled asphalt and the original asphalt is the proportion of internal macromolecular weight, the proportion of recycled asphalt's macromolecular weight is higher than original asphalt, that is, the carbonyl and sulfoxide group polar functional group contents are higher than original asphalt, so the rejuvenator has a significant improvement effect on aging asphalt but still cannot be fully restored to the state of the original asphalt.

3.6 AFM

In this section, the base asphalt, recycled asphalt, and aged asphalt are observed by using the atomic force microscope (AFMM), and the two-dimensional map of asphalt is obtained. Based on the change of bee-like structure, the improvement effect of the recycled agent on aged asphalt is analyzed. See Figure 12 for the two-dimensional diagram of six asphalts.

According to Figure 12, it is found that the two-dimensional diagrams of the six asphalts are all composed of non-bee-like and bee-like structures, and there is no essential change. Their morphologies are very similar, but there are some differences in the single bee-like structure and number. This shows that the rejuvenator and asphalt are simply physically dissolved, and there is no chemical reaction to produce new substances. This conclusion echoes the conclusion of the infrared spectrum mentioned earlier. Compared with the original asphalt, the number of bee-like structures of the aged asphalt decreases, while the size of a single structure increases. After adding the rejuvenator, the size of the single bee-like structure of aged asphalt decreases, but the number increases, and with the increasing amount of rejuvenator, this change continues to intensify.

The reason for this change lies in the aggregated state of the bee-like structure in asphalt is mainly influenced by the wax crystals and polar molecules in asphalt (Lv et al., 2019; Hong et al., 2020). From the experimental results of infrared spectroscopy, it is clear that after thermal-oxidative aging of asphalt, the asphalt molecules undergo chain-breaking and polymerization reactions to generate large molecules of polar functional groups such as carbonyl and sulfoxide groups as well as promoting the wax crystals, which also result in a decrease in the number of small molecules. As time grows, more and more polar molecules are gathered, finally, a bee-like molecular structure is formed. Therefore, the volume of the bee-like structure will become larger as the aging degree increases, and the number of bee-like structures is decreasing. At the same time, the force between the polar molecules is gradually increasing and the mobility is gradually decreasing, which makes the stiffness and complex modulus increase, the phase angle decreases, the stress relaxation time becomes longer, the stress gradually decreases, the creep rate decreases, and

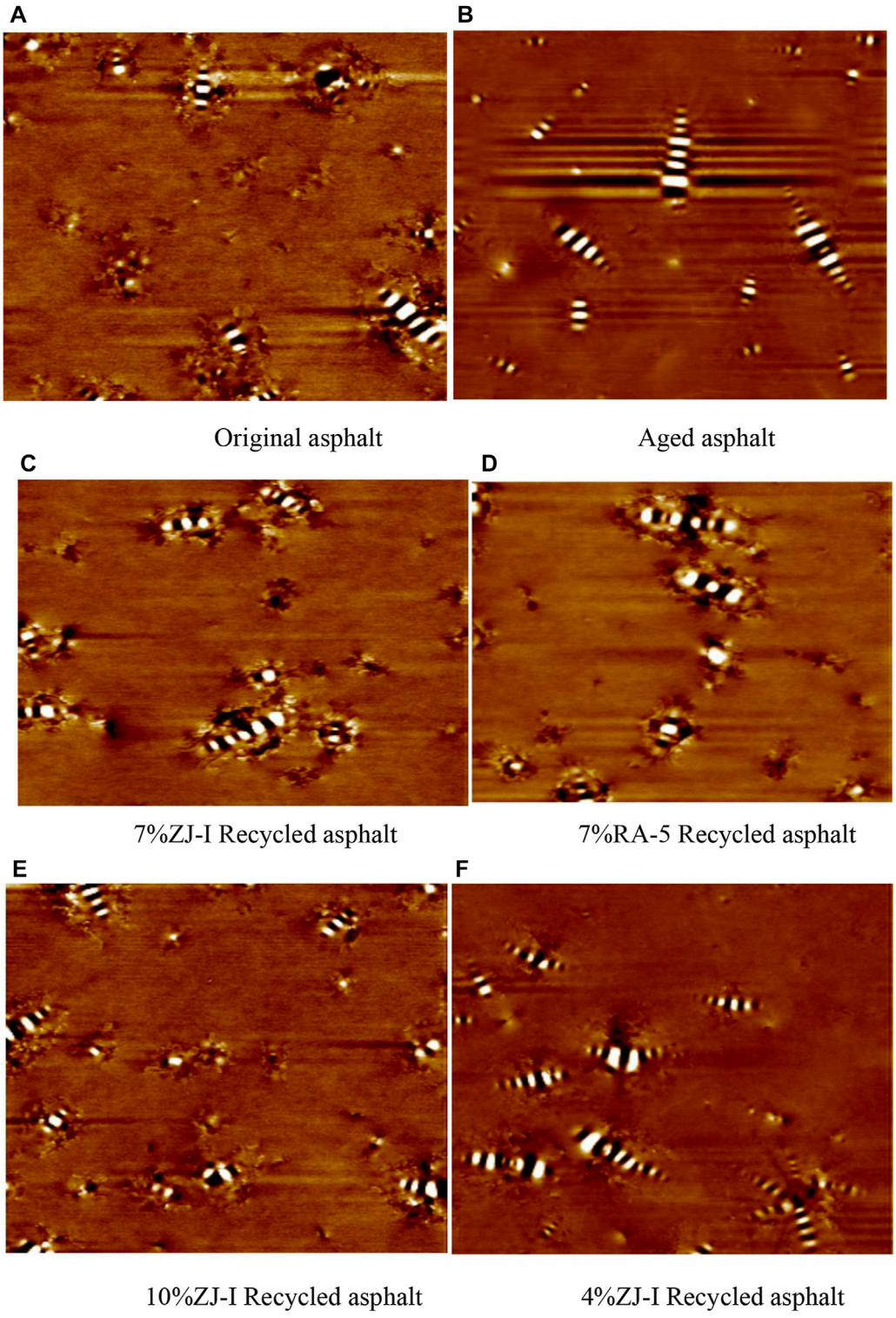

FIGURE 12
Two-dimensional AFM diagram of various asphalts.

TABLE 14 Contact angle of asphalt and liquid.

Materials	Distilled water	Ethylene glycol	Formamide
Recycled asphalt (10% ZJ-I)	90.70	65.30	70.41
Recycled asphalt (7% ZJ-I)	90.52	64.32	74.14
Recycled asphalt (4% ZJ-I)	92.00	67.79	76.89
Recycled asphalt (7% RA-5)	91.45	65.86	75.22
New asphalt	89.00	62.41	67.50
Aged asphalt	97.81	74.82	81.10

TABLE 15 Contact angle of aggregate with asphalt and water.

Aggregates	New asphalt	Aged asphalt	Recycled asphalt				Distilled water
			4% ZJ-I	7% ZJ-I	7% RA-5	10% ZJ-I	
Limestone	71.16	86.91	73.42	68.12	70.55	70.81	91.12

TABLE 16 Adhesion work and surface free energy.

Indicators	New asphalt	Aged asphalt	Recycled asphalt			
			4% ZJ-I	7% ZJ-I	10% ZJ-I	7% RA-5
Adhesion work (mJ\m^2)	38.59	21.99	29.77	34.73	36.08	32.71
Surface free energy (mJ\m^2)	29.172	20.872	23.16	25.302	27.153	24.536

finally the asphalt high-temperature shear ability increases and the low temperature crack resistance decreases.

The addition of the regenerating agent dissolves the aggregated polar molecules, making the polar molecules decompose into multiple small molecules, and to a certain extent, it inhibits the wax crystallization in asphalt, which leads to the enhancement of intermolecular mobility, the acceleration of the rate of asphalt release of temperature stress, the creep rate becomes larger, and finally, the area of the individual bee-like structure of asphalt becomes smaller and the number of bee-like structures becomes larger and significantly increases the low-temperature crack resistance of asphalt.

3.7 Adhesion

The results of the contact angle of aged asphalt, recycled asphalt, and original asphalt with liquid and the contact angle of aggregate with asphalt and water are shown in Table 14 and Table 15, respectively.

According to the data obtained in Table 14 and Table 15, combined with the formula, the surface free energy and adhesion work of asphalt can be obtained, and the results are shown in the following Table 16.

According to Table 16, it can be seen that the surface free energy of aged asphalt and the adhesion work between asphalt and aggregate are lower than the original asphalt and recycled asphalt. After adding the rejuvenator, the surface free energy of the aged asphalt and the adhesion work between asphalt and aggregate are significantly increased. With the increase of the rejuvenator content, the higher the values of the surface free energy of the regenerated asphalt and the adhesion work between asphalt and aggregate are. When the rejuvenator content is 10%, the surface free energy of the regenerated asphalt and the adhesion work between asphalt and aggregate are close to the original asphalt, but still slightly lower than the original asphalt. In addition, the surface free energy of the ZJ-I recycled asphalt and the adhesion work between asphalt and aggregate are slightly higher than RA-5 recycled asphalt when the content of the rejuvenator is 7%.

The reason for this phenomenon is that after the thermal oxygen aging of asphalt, the internal components of asphalt have changed, aromatic components, saturated components, and colloids have all been converted to asphaltene, and a large number of polar substances such as the maple group and carbonyl group have been generated, resulting in the reduction of surface free energy

of aging asphalt and adhesion work between asphalt and aggregate (Azarhoosh et al., 2018; Masri et al., 2021). However, after the rejuvenator is added, the rejuvenator dissolves the macromolecular weight, which reduces the surface tension of macromolecular segments in the aged asphalt, enhances the mobility between molecules, and reduces the polar components. Therefore, the surface free energy of the regenerated asphalt and the adhesion work between asphalt and aggregate gradually increase, approaching the original asphalt. However, the asphaltene of the ZJ-I regenerated asphalt is lower than the RA-5 regenerated asphalt and higher than the original asphalt. Therefore, the surface free energy of the ZJ-I recycled asphalt and the adhesion work between asphalt and aggregate are higher than the RA-5 recycled asphalt but lower than the original asphalt.

To sum up, through a series of macro and micro tests, it is found that the indexes of low-temperature and adhesion properties of asphalt with the 10% ZJ-I type rejuvenator are close to those of the original asphalt, but the high-temperature performance is worse than that with the 7% self-made ZJ-I type rejuvenator. Therefore, in order to take into account the high- and low-temperature performance and save costs, the optimal dosage of the rejuvenator is finally determined to be 7%.

4 Conclusion

In this paper, the formulation of the rejuvenator, as well as the regeneration effect and anti-aging property of the prepared rejuvenator were studied and evaluated by the results of different tests using dynamic shear rheology, bending creep stiffness, Fourier transform infrared spectroscopy, atomic force microscopy, and contact angle. The results showed that

1. Through the proportioning study, we get the ZJ-I rejuvenator's better performance formula as 83.6% extraction oil, 15% plasticizer DOP, 1.4% hydrogenated petroleum resin, 0.6% antioxidant, and 0.4% light stabilizer
2. Aging asphalt with ZJ-I rejuvenator dosing improves the rheological properties of recycled asphalt, but at the same time will lead to high-temperature shear resistance decay
3. ZJ-I rejuvenator admixture dissolved the large molecular weight of carbonyl and sulfoxide groups and other polar functional groups, thus alleviating the degree of aging asphalt, but not fully restored to the level of the original asphalt
4. After adding the ZJ-I regenerating agent, the area of the individual bee-like structure of the regenerated asphalt gradually decreases, and the number of bee-like structures increases, which makes the large molecular weight content decrease, thus alleviating the aging degree
5. After adding the ZJ-I rejuvenator, the free energy of the asphalt surface and adhesion work increased, thus enhancing the adhesion of asphalt and aggregate, and finally, the best dosing of the ZJ-I rejuvenator was determined to be 7% (Shao-peng et al., 2002; Radzi et al., 2020; Sharma et al., 2020; Elio et al., 2021; Yin and Pan, 2022; Han et al., 2022)

Data availability statement

The original contributions presented in the study are included in the article/Supplementary Material; further inquiries can be directed to the corresponding author.

Author contributions

JY: first draft writing; XY: thesis review; and LZ: experimental data collation.

Conflict of interest

LZ was empolyed by Xinjiang Beixin Investment and Construction Co.

The remaining authors declare that the research was conducted in the absence of any commercial or financial relationships that could be construed as a potential conflict of interest.

Publisher's note

All claims expressed in this article are solely those of the authors and do not necessarily represent those of their affiliated organizations, or those of the publisher, the editors, and the reviewers. Any product that may be evaluated in this article, or claim that may be made by its manufacturer, is not guaranteed or endorsed by the publisher.

References

Al-Saffar, Z. H., Yaacob, H., Idham, M. K., Jaya, R. P., Hassan, N. A., Radeef, H. R., et al. (2021). Evaluating the performance of reclaimed asphalt pavement incorporating PelletRAP as a rejuvenator[C]. *IOP Conf. Ser. Earth Environ. Sci.* 682 (1), 012068. IOP Publishing. doi:10.1088/1755-1315/682/1/012068

Al-Saffar, Z. H., Yaacob, H., Mohd Satar, M. K. I., and Putra Jaya, R. (2022). The tailored traits of reclaimed asphalt pavement incorporating maltene: Performance analyses. *Int. J. Pavement Eng.* 23 (6), 1800–1813. doi:10.1080/10298436.2020.1824294

AlSaffar, Z. H., Yaacob, H., Saleem, M. K., Mohd Satar, M. K. I., Putra Jaya, R., Bilema, M., et al. (2022). A new approach to enhance the reclaimed asphalt pavement features: Role of maltene as a rejuvenator. *Road Mater. Pavement Des.* 23 (11), 2507–2530. doi:10.1080/14680629.2021.1984978

Azarhoosh, A., Nejad, F. M., and Ali, K. (2018). Evaluation of the effect of nano-TiO2 on the adhesion between aggregate and asphalt binder in hot mix asphalt. *Eur. J. Environ. Civ. Eng.* 22 (8), 946–961. doi:10.1080/19648189.2016.1229227

Elio, Z., Fateh, F. T., Alain, B., Christophe, P., Joseph, A., Anne, M., et al. (2021). Experimental and numerical investigation on the rheological behaviour of bituminous composites via DSR testing. *Road Mater. Pavement Des.* 22 (S1), S328–S344. doi:10.1080/14680629.2021.1912812

Gao, F., and Wang, N. (2016). "The structural design and relevant calculations of 4000 asphalt recycler," in 6th international conference on information engineering for mechanics and materials, 42–47. Atlantis Press. doi:10.2991/icimm-16.2016.9

Gómez-Mejide, B., Ajam, H., Lastra-González, P., Garcia, A., et al. (2018). Effct of ageing and RAP content on the induction healing propertis of asphalt mixtures. *Constr. Build. Materilas* 17 (09), 468–476. doi:10.1016/j.conbuildmat.2018.05.121

Han, Y., Cui, B., Tian, J., Ding, J., Ni, F., and Lu, D. (2022). Evaluating the effects of styrene-butadiene rubber (SBR) and polyphosphoric acid (PPA) on asphalt adhesion performance. *Constr. Build. Mater.* 321, 126028. doi:10.1016/j.conbuildmat.2021.126028

Hong, W., Mo, L., Pan, C., Riara, M., Wei, M., and Zhang, J. (2020). Investigation of rejuvenation and modification of aged asphalt binders by using aromatic oil-SBS polymer blend. *Constr. Build. Mat.* 231, 117154. doi:10.1016/j.conbuildmat.2019.117154

Huang, B., Ma, Y., Wang, S., Zhou, H., Hu, W., and Polaczyk, P. (2021). Potential alternative to styrene–butadiene–styrene for asphalt modification using recycled rubber–plastic blends. *J. Mater. Civ. Eng.* 33 (12), 04021341. doi:10.1061/(ASCE)MT.1943-5533.0003946

Huang, S. L., Shen, F., and Ding, Q. J. (2011). Research on the application of recycled PE in high modulus asphalt mixture. In advanced materials research *Trans Tech Publications Ltd.* 287, 1155–1163. doi:10.4028/www.scientific.net/AMR.287-290.1155

Jaafar, Z. F. M., Ramadhansyah, P. J., Masri, K. A., Mashros, N., Warid, M. N. M., Norhidayah, A. H., et al. (2021). The effects of nano kaolin clay modified bitumen on the softening point and storage stability[C]. *IOP Conf. Ser. Earth Environ. Sci.* 682 (1), 012062. IOP Publishing. doi:10.1088/1755-1315/682/1/012062

Li, L., Li, Y., and Huang, J. (2022). Quantifying the effect of hot recycling on asphalt mixtures based on rod thin-layer chromatography. *J. Test Eval.* 50 (5). doi:10.1520/JTE20210705

Li, P., Mu, B., Nian, T., Mao, Y., Tang, J., and Li, J. H. (2022). Positional behavior and substrate use in wild Tibetan macaques. *Animals.* 40 (05), 767–773+784. doi:10.3390/ani12060767

Liu, Y. L., Zhao, N., and Zhao, J. (2012). The durability analysis of secondary recycled asphalt mixture. In advanced materials research *Trans Tech Publications Ltd.* 557, 1497–1500. doi:10.4028/www.scientific.net/AMR.557-559.1497

Lv, X., Fan, W., Wang, J., Liang, M., Qian, C., Luo, H., et al. (2019). Study on adhesion of asphalt using AFM tip modified with mineral particles. *Constr. Build. Mater.* 207, 422–430. doi:10.1016/j.conbuildmat.2019.02.115

Masri, K. A., Syafiqah, S. M. Z. N., Seman, M. A., Jaya, R. P., Yaacob, H., and Mashros, N. (2021). A review on nanomaterials as additive in asphalt binder[C]. *IOP Conf. Ser. Earth Environ. Sci.* 682 (1), 012055. IOP Publishing. doi:10.1088/1755-1315/682/1/012055

Nie, X., Hou, T., Yao, H., Zheng, L., Zhou, X., and Li, C. (2019). Effect of C9 petroleum resins on improvement in compatibility and properties of SBS-modified asphalt. *Petroleum Sci. Technol.* 37 (14), 1704–1712. doi:10.1080/10916466.2019.1602642

Radzi, N. A. M., Masri, K. A., Ramadhansyah, P. J., Jasni, N. E., Arshad, A. K., Ahmad, J., et al. (2020). Stability and resilient modulus of porous asphalt incorporating steel fiber[C]//IOP conference series: Materials science and engineering. *IOP Conf. Ser. Mat. Sci. Eng.* 712 (1), 012027. doi:10.1088/1757-899x/712/1/012027

Sharma, V. K., Kumar, V., and Singh Joshi, R. (2020). Parametric study of aluminium-rare Earth based composites with improved hydrophobicity using response surface method. *J. Mater. Res. Technol.* 9 (03), 4919–4932. doi:10.1016/j.jmrt.2020.03.011

Shao-peng, W., Xiao-ming, H., and Yong-li, Z. (2002). The development of recycling agent for asphalt pavement. *J. of Wuhan University of Technology-Mater. Sci.* 17 (65, 63–65. doi:10.1007/BF02838543

Sokolova, M. D., Fedorova, A. F., and Pavlova, V. V. (2019). Research of influence of plasticizers on the low-temperature and mechanical properties of rubbers. *Mater. Sci. Forum* 945, 459–464. doi:10.4028/www.scientific.net/msf.945.459

Walubita Lubinda, F., Luis, F., Hossain, T., Chunduri Harshavardhan, R., and Samer., D. (2021). Correlating the asphalt-binder BBR test data to the HMA (ML-OT) fracture properties. *J. Mat. Civ. Eng.* 33 (9). doi:10.1061/(asce)mt.1943-5533.0003866

Wang, F. L., Long, J., Shen, B. X., and Ling, H. (2014). A Study of the regenerating effects of recycling agents on aged asphalts. *Petroleum Science and Technology* 32 (10), 1160–1167. doi:10.1080/10916466.2011.616566

Wu, H., Peng, C., Chen, C., and Zhang, W. (2022). Effect of aromatic petroleum resin on microstructure of SBS modified asphalt. *Adv. Mater. Sci. Eng.* 2022, 1–11. doi:10.1155/2022/5136748

Wu, W-L., and Dai, S-L. (2022). Study on the rheological and temperature-sensitive properties of furfural extracted oil recycled asphalt. *J. Zhengzhou Univ. Eng. Ed.* 43 (03), 52–58+66.

Xiao, F., Yao, S., Wang, J., Li, X., and Amirkhanian, S. (2018). A literature review on cold recycling technology of asphalt pavement. *Constr Build Mater.* 180, 579–604. doi:10.1016/j.conbuildmat.2018.06.006

Yanan, C., Cui, S., and Guo, L. (2022). Performance and mechanism of SBS modified asphalt regenerated by waste engine oil. *J. Constr. Mater.* 25 (02), 164–170.

Yin, P., and Pan, B. (2022). Evaluation of temperature sensitivity of recycled asphalt based on numerical analysis model and thermal analysis kinetics. *Constr. Build. Mater.* 344, 128153. doi:10.1016/j.conbuildmat.2022.128153

Zhao, H., Su, J., Ma, S., Su, C., Wang, X., Li, Z., et al. (2022). Study on cold recycled asphalt mixtures with emulsified/foamed asphalt in the laboratory and on-Site. *Coatings* 12 (7), 1009. doi:10.3390/coatings12071009

Zhu, H. Z., Yan, E. H., and Lu, Z. T. (2017). Evaluation of fatigue performance of asphalt based on constant strain DSR test. *IOP Conf. Ser. Mat. Sci. Eng.* 170 (1), 012003. doi:10.1088/1757-899x/170/1/012003